'94 KACC (1994. 10. 17 ~ 20)

Lumped-Parameter Modeling of Flexible Manipulator Dynamics

Jin-Soo Kim Atsushi Konno Masaru Uchiyama Kazuaki Usui
Kazuki Yoshimura
Department of Aeronautics and Space Engineering,
Tohoku University
Aramaki-aza-Aoba, Aoba-ku, Sendai 980-77, Japan

Abstract

In this paper, we discuss the modeling of flexible manipulators. In the modeling of flexible manipulators, there are two approaches: one is based on the distributed-parameter modeling and the other on the lumped-parameter modeling. The former has been applied to control and analysis of simple manipulator requiring precision, while the latter has been applied to multi-link spatial manipulator, because of the model's simplicity. We have already proposed the lumped-parameter modeling method for a multi-link spatial flexible manipulators. In this paper, we apply our lumped-parameter modeling method for simple manipulator, and investigate that model of how much degree of precision we can get. The experiments and simulations are performed, comparing these results, the approximate performance of our modeling method is discussed.

1 Introduction

Because of the rapid development of industrial automation, robot of high speed, lightweight and saving energy are required. Also, in the field of space applications, these properties are demanded. The main problem with lightweight manipulators is the tip deflection and the structural vibration due to the elasticity of arm's component parts. The problems motivate the growing interest in research on flexible manipulators.

The research on flexible manipulators began about 1970 and since then, it has been a subject of a number of publications. Among these publications, the modeling of flexible manipulators has been one of the main theme of research [1]~[3]. The opening research had mainly centralized upon the planar one-link or two-link flexible manipulators and had been applying distributed-parameter modeling for those manipulators. The dynamic equation of motion had been derived by using the partial differential equation [1]. However, due to the complexity, only few attempts have been made so far for the distributed-parameter model of multi-link, multi-DOF spatial flexible manipulators [2]. Therefore, there has been renewal of interest in the lumped-parameter modeling in recent years [4]~[6].

In some multi-link spatial flexible manipulators, equations of motion depend upon arm's configuration, and thus, simple models are required for real time computation. Lumped-parameter models are effective for such purpose [4][5]. On the contrary, in control of one or two link planar flexible structure (e.g. solar paddle), since equations of motion change little depending upon structure's configuration, precise models are more desirable than simple models.

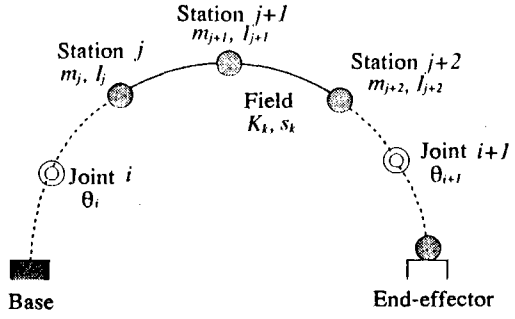

Fig. 1: A Lumped-mass and spring model of flexible manipulator.

Our aim is to develop a modeling method which is applicable for both purposes. We have already proposed a modeling method for multi-link spatial flexible manipulators [5]. In this paper, we prove that our modeling method can be applied to the model requiring precision. The effectiveness of our modeling method is discussed by comparing the natural frequencies and the amplitudes of simulation results with those of experimental results.

2 A Lumped-Mass and Spring Model

In this section, our proposed modeling method [5] is briefly explained. The method assumes that the mass of system is concentrated at chosen points, called *stations*, whereas the segments between two stations, called *fields*, are massless and elastic in property.

The term *station* and *field* are originally used in Holzer's modeling method [7].

Fig. 1 shows our proposed model of a flexible manipulator [5], where station is defined by mass m_j and inertia I_j ($j = 1, 2 \cdots, p$), while field is defined by stiffness

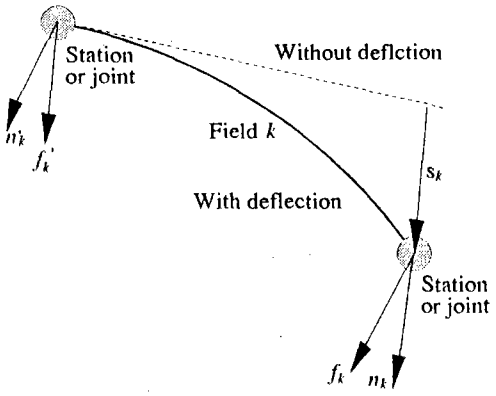

Fig. 2: Forces, moments and deflections at the kth field.

k_k ($k = 1, 2 \cdots, q$). Displacement of a station from it's nominal position is given by elastic deflection vector $\boldsymbol{s}_k$ (**Fig. 2**). Generally, $\boldsymbol{s}_k$ is a 6-dimensional vector that represents the linear and angular deflection. The overall elastic deflection vector $\boldsymbol{e}$ can be written in the following form

$$\begin{aligned} \boldsymbol{e} &= \left[\begin{array}{cccc} \boldsymbol{s}_1^T & \boldsymbol{s}_2^T & \cdots & \boldsymbol{s}_q^T \end{array} \right]^T \\ &= \left[\begin{array}{cccc} e_1 & e_2 & \cdots & e_m \end{array} \right]^T, \end{aligned} \tag{1}$$

where $m = 6q$. Let $\boldsymbol{f}_k$, $\boldsymbol{n}_k$ respectively be the force and moment of one side of the k-th field. The prime means the other side. The relation between $\boldsymbol{f}_k$, $\boldsymbol{n}_k$ and $\boldsymbol{s}_k$ can be expressed as

$$\left[\begin{array}{c} \boldsymbol{f}_k \\ \boldsymbol{n}_k \end{array} \right] = \boldsymbol{K}_k \boldsymbol{s}_k, \tag{2}$$

where $\boldsymbol{K}_k$ is the stiffness matrix of k-th field. We apply the modeling method to a one-link planar flexible manipulator in the next section.

3 Modeling of One-Link Flexible Manipulator

3.1 A Lumped-Mass and Spring Model

Fig. 3 shows a lumped-mass and spring model of a one-link planar flexible manipulator. The coordinate system of the flexible manipulator considered in this paper is shown in **Fig. 3**. $x - y$ coordinate frame is stationary and $x' - y'$ coordinate frame rotates with the hub of manipulator. In this figure, θ is hub angle, δ_k is elastic deflection, and ϕ_k is elastic angular deflection. Herein, $\boldsymbol{s}_k$ and $\boldsymbol{e}$ in Eq. (1) can be written as

$$\begin{aligned} \boldsymbol{s}_k &= \left[\begin{array}{cc} \delta_k & \phi_k \end{array} \right]^T, \\ \boldsymbol{e} &= \left[\begin{array}{cccc} \delta_1 & \phi_1 & \delta_2 & \phi_2 \cdots \end{array} \right]^T. \end{aligned} \tag{3}$$

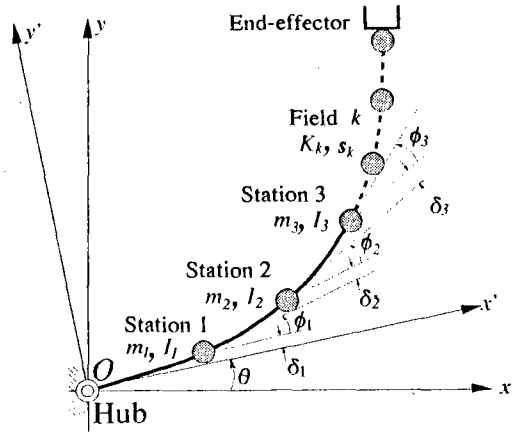

Fig. 3: Lumped-mass and spring model of a one-link flexible manipulator.

$\boldsymbol{K}_k$ in Eq. (2) can also be written as

$$\boldsymbol{K}_k = \left[\begin{array}{cc} \frac{12E_kI_k}{l_k^3} & -\frac{6E_kI_k}{l_k^2} \\ -\frac{6E_kI_k}{l_k^2} & \frac{4E_kI_k}{l_k} \end{array} \right], \tag{4}$$

where E_kI_k and l_k are respectively stiffness and length of field.

3.2 Equations of Motion

Equations of motion are derived by Lagrange's method. Let $\boldsymbol{r}_j(\theta, \boldsymbol{e})$ be the position vector of j-th station. The overall kinematic energy T and potential energy U of the manipulator can be respectively written as

$$T = \frac{1}{2} \sum_{j=1}^{p} \left(m_j \dot{\boldsymbol{r}}_j^T \dot{\boldsymbol{r}}_j + I_j \dot{\phi}_j^2 \right) + \frac{1}{2} I_a \dot{\theta}^2, \tag{5}$$

$$U = \frac{1}{2} \boldsymbol{e}^T \boldsymbol{K}_{22} \boldsymbol{e} - \sum_{j=1}^{p} \left(m_i \boldsymbol{r}_j^T \boldsymbol{g} \right), \tag{6}$$

where $\boldsymbol{K}_{22} = \mathrm{diag}(\boldsymbol{K}_1 \cdots \boldsymbol{K}_q)$, I_a is the the rotor's inertia of the actuator. We consider the manipulator's motion in the horizontal plane, thus the effect of gravity can be neglected. The Lagrangian L is

$$\begin{aligned} L &= T - U \\ &= \sum_{i=1}^{p} \left(\frac{1}{2} m_j \dot{\boldsymbol{r}}_j^T \dot{\boldsymbol{r}}_j + \frac{1}{2} I_j \dot{\phi}_j^2 \right) + \frac{1}{2} I_a \dot{\theta}^2 - \frac{1}{2} \boldsymbol{e}^T \boldsymbol{K}_{22} \boldsymbol{e}. \end{aligned} \tag{7}$$

Using Eq. (7), we obtain the equations of motion as follows:

$$\tau = \frac{d}{dt} \left(\frac{\partial L}{\partial \dot{\theta}} \right) - \frac{\partial L}{\partial \theta}, \tag{8}$$

$$\mathbf{o} = \frac{d}{dt} \left(\frac{\partial L}{\partial \dot{e}_i} \right) - \frac{\partial L}{\partial e_i}, \tag{9}$$

where τ is joint torque. Transforming Eqs. (8) and (9) into matrix form, we obtain

$$\left[\begin{array}{c} \tau \\ \mathbf{0} \end{array} \right] = \left[\begin{array}{cc} \boldsymbol{M}_{11}(\theta, \boldsymbol{e}) & \boldsymbol{M}_{12}(\theta, \boldsymbol{e}) \\ \boldsymbol{M}_{21}(\theta, \boldsymbol{e}) & \boldsymbol{M}_{22}(\theta, \boldsymbol{e}) \end{array} \right] \left[\begin{array}{c} \ddot{\theta} \\ \ddot{\boldsymbol{e}} \end{array} \right]$$

$$+\begin{bmatrix} h_1(\theta,\dot{\theta},e,\dot{e}) \\ h_2(\theta,\dot{\theta},e,\dot{e}) \end{bmatrix}+\begin{bmatrix} 0 & 0 \\ 0 & K_{22} \end{bmatrix}\begin{bmatrix} \theta \\ e \end{bmatrix}, \quad (10)$$

or in a compact form

$$M\ddot{q}+h+Kq=L\tau, \quad (11)$$

where

$$q=\begin{bmatrix} \theta \\ e \end{bmatrix}, \quad L=\begin{bmatrix} 1 \\ 0 \end{bmatrix}.$$

3.3 Modal Analysis

The equation which is related to the elastic motion can be separated from Eq. (10) as

$$\ddot{e}+M_{22}^{-1}K_{22}e=-M_{22}^{-1}M_{21}\ddot{\theta} \quad (12)$$

Let's consider the modal decomposition. The eigenvalues and eigenvectors of $M_{22}^{-1}K_{22}$ are given by

$$M_{22}^{-1}K_{22}\Psi_r=\Omega_r\Psi_r \quad (r=1,2,\cdots,m) \quad (13)$$

The deflection vector e can be expressed by a linear combination of the eigenvectors and the modal coordinates as

$$\begin{aligned} e &= \sum_{r=1}^{m}\Psi_r e_r^*, \\ &= \Psi e^* \end{aligned} \quad (14)$$

where Ψ and e^* are respectively the modal matrix and the modal coordinate, and are represented as

$$\begin{aligned} \Psi &= \left[\ \Psi_1,\ \Psi_2,\ \cdots,\ \Psi_m\ \right], \\ e^* &= \left[\ e_1^*,\ e_2^*,\ \cdots,\ e_n^*\ \right]^T. \end{aligned} \quad (15)$$

4 Simulation and Experiment

In this section, the effectiveness of our modeling method is discussed. For that purpose, applying our modeling method, three kinds of lumped-mass and spring models of our experimental flexible manipulator are constructed. Based on these models, simulations are performed. These results, based on a precise model constructed by commercial dynamic analysis software packages, are compared with experimental results.

4.1 Experimental Setup

Fig. 4 shows an overview of our experimental flexible manipulator (FLEBOT 0). The manipulator is composed of one elastic link and one rotary joint. Rotary joint is actuated by DC servo motor with hardware velocity feedback. Joint velocity is measured by tachometer. A shaft potentiometer is used as the sensor of hub angle, while a laser beam and a PSD (Position Sensitive Device) is used to measuer the tip deflection of the arm. **Table 1** lists the properites of FLEBOT 0.

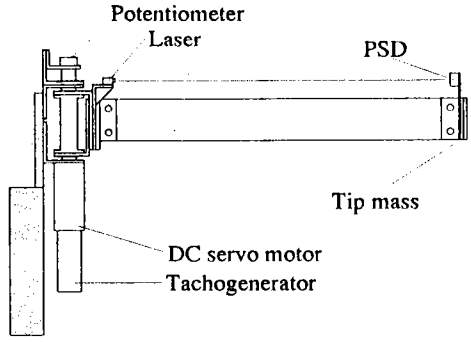

Fig. 4: Overview of the experimental flexible manipulator FLEBOT 0.

Table 1: Properites of FLEBOT 0.

Parameter	Notation	Value
Length of the link	l [m]	0.50
Stiffness of the link	EI [Nm^2]	6.2034
Roter's inertia	I_a [kgm^2]	3.1458×10^{-2}
Reduction ratio	G_r	88
Mass of the link	m_1 [kg]	0.37
Mass of the tip	m_2 [kg]	0.5744 or 0.8774

4.2 Control Scheme

FLEBOT 0 is equipped with the velocity servo motor with hardware velocity feedback system. The joint motion is commanded by joint velocity command. Thus, joint torque cannot be controlled directly. Here, we assume the relationship between velocity command and the produced torque as follows:

$$\begin{aligned} \tau &= G_r K_{sp}(V_{ref}-K_{sv}\dot{\theta}_m), \\ &= \Lambda(\dot{\theta}_c-\dot{\theta}), \end{aligned} \quad (16)$$

where

G_r	is the gear reduction ratio,
K_{sp}	is the voltage feedback gain,
K_{sv}	is the voltage/velocity coefficent,
$\dot{\theta}_m = G_r\dot{\theta}$	is the angular velocity of motor,
V_{ref}	is the voltage corresponding to the velocity command,
$\dot{\theta}_c$	is the velocity command, and
$\Lambda = G_r^2K_{sp}K_{sv}$	is the velocity feedback gain.

We consider simple P-control for joint motion. Velocity command $\dot{\theta}_c$ is computed by

$$\dot{\theta}_c=-F_{pt}(\theta-\theta_d), \quad (17)$$

where F_{pt} is an appropriate gain. Voltage velocity command V_{ref} is computed by

$$V_{ref}=G_rK_{sv}\dot{\theta}_c, \quad (18)$$

and used in the experiments. Eq. (17) can be rewritten as:

$$\begin{aligned} \dot{\theta}_c &= -\begin{bmatrix} 0 & 0 & F_{pt} & 0 \end{bmatrix}\begin{bmatrix} \dot{q}-\dot{q}_d \\ q-q_d \end{bmatrix}, \\ &= -Fx \end{aligned} \quad (19)$$

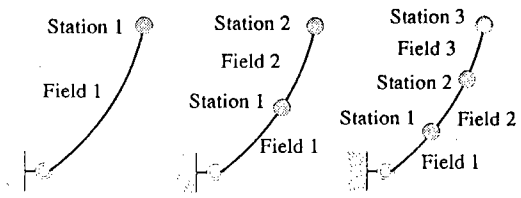

Fig. 5: Constructed models.

In order to simplify Eqs. (10) and (11) we make the following assumptions:

- Firstly, we will only consider the slow motion, and thus, the centrifugal and Corioli's forces can be neglected,

$$\boldsymbol{h}(\boldsymbol{q}, \dot{\boldsymbol{q}}) = \boldsymbol{0},$$

- Secondly, we will assume that the influence of elastic deflection $\boldsymbol{e}$ in the inertia matrix is small, and thus,

$$\boldsymbol{M}(\theta, \boldsymbol{e}) \approx \boldsymbol{M}(\theta).$$

Substituting Eq. (16) in Eq. (11), along with above assumptions, we have

$$\boldsymbol{M}\ddot{\boldsymbol{q}} + \boldsymbol{L}\Lambda\boldsymbol{L}^T\dot{\boldsymbol{q}} + \boldsymbol{K}\boldsymbol{q} = \boldsymbol{L}\Lambda\dot{\theta}_c. \tag{20}$$

In this case the desired states are

$$\boldsymbol{q}_d = \begin{bmatrix} \theta_d \\ \boldsymbol{e}_d \end{bmatrix} = \begin{bmatrix} \theta_d \\ \boldsymbol{0} \end{bmatrix}, \quad \dot{\boldsymbol{q}}_d = \ddot{\boldsymbol{q}}_d = \begin{bmatrix} 0 \\ \boldsymbol{0} \end{bmatrix}, \tag{21}$$

therefore, Eq. (20) can be transformed into the state-space form as

$$\begin{bmatrix} \ddot{\boldsymbol{q}} - \ddot{\boldsymbol{q}}_d \\ \dot{\boldsymbol{q}} - \dot{\boldsymbol{q}}_d \end{bmatrix} = \begin{bmatrix} -\boldsymbol{M}^{-1}\boldsymbol{L}\Lambda\boldsymbol{L}^T & -\boldsymbol{M}^{-1}\boldsymbol{K} \\ \boldsymbol{I} & \boldsymbol{0} \end{bmatrix} \times \begin{bmatrix} \dot{\boldsymbol{q}} - \dot{\boldsymbol{q}}_d \\ \boldsymbol{q} - \boldsymbol{q}_d \end{bmatrix} + \begin{bmatrix} \boldsymbol{M}^{-1}\boldsymbol{L}\Lambda \\ \boldsymbol{0} \end{bmatrix} \dot{\theta}_c. \tag{22}$$

Eq. (22) can be cast into state equation form as follows:

$$\dot{\boldsymbol{x}} = \boldsymbol{A}\boldsymbol{x} + \boldsymbol{B}\dot{\theta}_c. \tag{23}$$

In the simulations, the discrete-time state equation corresponding to Eq. (23) is used in the following form:

$$\boldsymbol{x}(k+1) = \boldsymbol{\Phi}\boldsymbol{x}(k) + \boldsymbol{\Gamma}\dot{\theta}_c(k), \tag{24}$$

where k indicates the k-th interval of the sampling process, $\boldsymbol{\Phi}$ and $\boldsymbol{\Gamma}$ are the discrete matrices of $\boldsymbol{A}$ and $\boldsymbol{B}$ for a zero-order holder (ZOH).

4.3 A Precise Model

A precise model of FLEBOT 0 is constructed by ADAMS™. ADAMS™ is a commercial software package for dynamic analysis of mechanical systems produced by Mechanical Dynamics, Incorporated. In this simulator, a finite-element method based on Timoshenko beam theory is used as a modeling method of flexible structure. In order to obtain a precise model, the elastic beam is divided into ten pieces, here. We consider our experimental manipulator as having 10 beam elements.

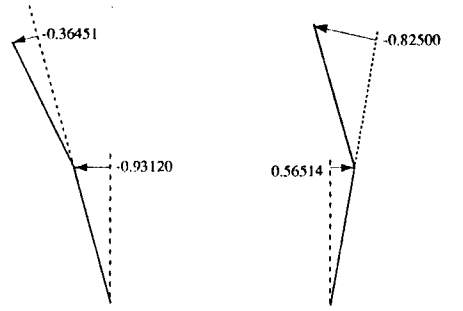

Fig. 6: 2 stations vibration mode shapes.

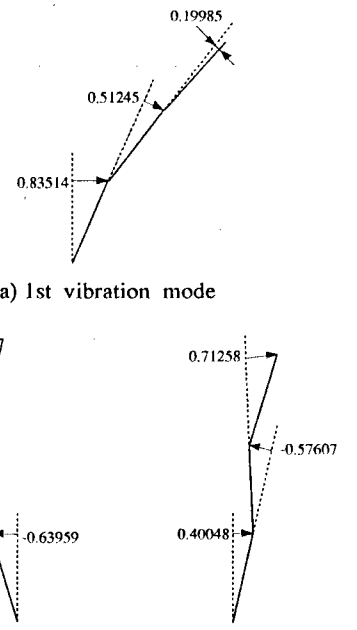

Fig. 7: 3 stations vibration mode shapes.

4.4 Models Based on Our Modeling Method

Three kinds of models of FLEBOT 0 based on our modeling method are constructed: a) one station model, b) two station model, and c) three station model (**Fig. 5**). Based on these models, simulations are performed on MATLAB™ software package (The Math Works, Incorporated's product). Mode shapes of two station model and three station model can be obtained by computing the modal matrix $\boldsymbol{\Psi}$, and drawn in **Fig. 6** and **Fig. 7**.

4.5 Results and Discussion

The response results for step input of desired angle are computed by the two simulators and experimented by the flexible manipulator. Furthermore, both results for

Table 2: Comparing frequencies of the simulation.

Type	[Hz] ($m_2 = 0.8774$)		
	1st mode	2nd mode	3rd mode
1 station (MATLAB)	1.7388		
2 station (MATLAB)	1.8682	27.536	
3 station (MATLAB)	1.9073	28.745	84.260
ADAMS	2.0265	29.692	89.708

Table 3: Computed natural frequencies of 1st mode.

Type	[Hz] ($m_2 = 0.5744$)	[Hz] ($m_2 = 0.8774$)
1 station	1.9983	1.7388
2 station	2.2023	1.8682
3 station	2.267	1.9073
ADAMS	2.4876	2.0267
Expriment	2.4938	2.0492

the one link flexible manipulator are used to verify our modeling method. In the experiment and simulation, we set $F_{pl} = 2\,(s^{-1})$ and the sampling time as 10 (ms). For these simulations, K_{ep} of Eq. (16) is decided to be approximated to the experimental results.

The results of simulations and experiments are shown in **Fig. 8** and **9**. **Fig. 8** and **Fig. 9** respectively show the responses of joint motion and elastic deflection at the tip. Natural frequencies of one station model, two station model and three station model are computed from the eigenvalues of $\boldsymbol{A}$ in Eq. (23). Computed natural frequencies of our models and the precise models analyzed on ADAMS™ software are presented in **Table 3**. Natural frequencies of the 1st vibration mode computed from each model are compared with the experimental results and presented in **Table 2**

Fig. 8, **Fig. 9** and **Table 3** point out that in case of the tip mass being larger than the link mass, our modeling method is proper for only a few number of stations and fields, but in contrast, in case of the tip mass being smaller than the link mass, our modeling method is proper only for a considerable number of stations and fields. Therefore, dividing the flexible manipulator into a suitable number of stations and fields is needed for our modeling method to be very effective. Suitable number of stations and fields is decided by the charater of manipulator, the controller and the requisite precision. For example, in case of flexible manipulators with quite high flexibility, its model needs a considerably large number of stations and fields to obtain a precise model.

5 Conclusions

One-link planar flexible manipulator has been modeled by using a lumped-parameter modeling method. Experimental results show that the system responses are in good agreement with simulation results. Investigating these results, it can be concluded that our modeling method is effective not only to construct a simple model for multi-link flexible manipulators, but also to construct a precise model for one-link flexible manipulators, space flexible structures and so on.

Future work in this area will find a formula which can decide a suitable number of stations and fields for flexible manipulators.

References

[1] R. H. Cannon Jr. and E. Schmitz, "Initial experiments on the end-point control of a flexible one-link robot," Int. J. of Robotics Research, Vol. 3, No. 3, pp. 62–75, 1984.

[2] W. H. Sunada and S. Dubowsky, "On the dynamic analysis and behavior of industrial robotic manipulators with elastic members," Trans. of ASME, J. of Mechanisms, Transmissions, and Automation in Design, Vol. 105, pp. 42–51, 1983.

[3] E. Bayo, "A finite-element approach to control the end-point motion of a single-link flexible robot," J. of Robotic Systems, Vol. 4, No. 1, pp. 63–75, 1987.

[4] T. Yoshikawa, H. Murakami, and K. Hosoda, "Modeling and Control of a Three Degree of Freedom Manipulator with Two Flexible Links," Proc. of the 29th IEEE Conf. on Decision and Control, pp. 2532-2537, 1990

[5] M. Uchiyama and A. Konno, "Modeling of the Flexible Arm Dynamics Based on the Holzer's Method," Proc. RSJ 1st Robotics Symposium, pp. 247-252, 1991 (In Japanese).

[6] J. S. Kim, M. Uchiyama, A. Konno, K. Usui, and K. Yoshimura, "Modeling of Flexible Manipulator Dynamics," JSME Design and Dynamics Conference, Vol. B, pp. 57-60, 1993 (In Japanese).

[7] L. Meirovitch, Analytical Methods in Vibrations, Macmillan Publishing Co., Inc., 1967.

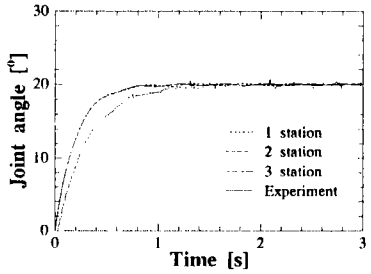

(a) Mass of the tip is 0.5744 (kg).

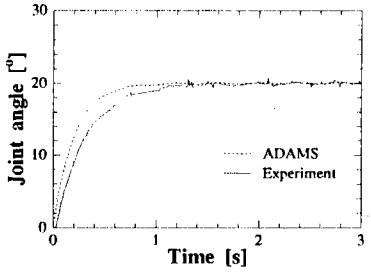

(b) Mass of the tip is 0.5744 (kg).

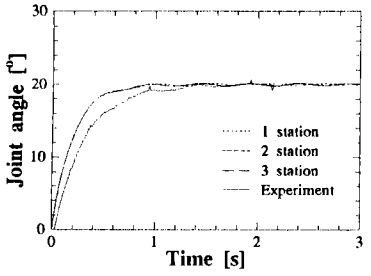

(c) Mass of the tip is 0.8774 (kg).

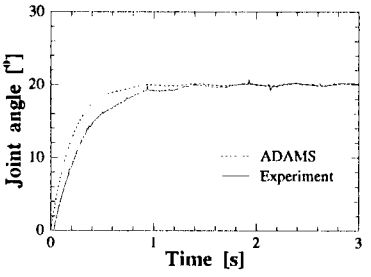

(d) Mass of the tip is 0.8774 (kg).

Fig. 8: Joint respones.

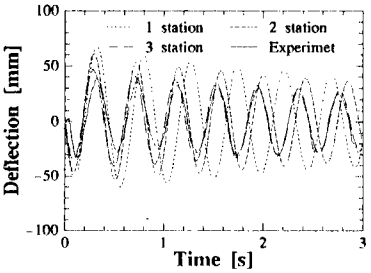

(a) Mass of the tip is 0.5744 (kg).

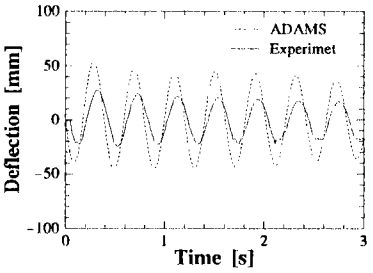

(b) Mass of the tip is 0.5744 (kg).

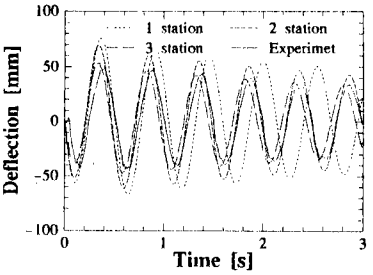

(c) Mass of the tip is 0.8774 (kg).

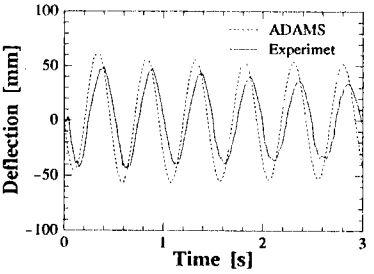

(d) Mass of the tip is 0.8774 (kg).

Fig. 9: Tip displacements.